

Solar Air Conditioning with Metal Organic Frameworks

Undergraduate Honors Thesis

Presented in Partial Fulfillment of the Requirements for the Undergraduate Research

Distinction in the Mechanical Engineering School at The Ohio State University

By

James Albert Staschiak

The Ohio State University

2020

Advisor: Dr. Jordan D. Clark

Copyrighted by
James Albert Staschiak
2020

Abstract

Air conditioning is responsible for 5% of energy consumption in the United States as is increasingly in demand across the world as the global middle class continues to grow in size. During hotter months, electricity used to power cooling systems becomes taxing on electric grids, constituting approximately 40% of peak power demand. Traditional air conditioning (AC) systems are also associated with harmful environmental impacts. Both refrigerants used for cooling and fossil fuels used in power contribute to global warming by acting as green-house gases (GHG). Due to the negative effects associated with emissions, the ultimate goal of this research is to drastically reduce non-renewable energy consumption associated with AC units. Generations of technologies have been developed to address this ongoing issue. An emerging solution involves the integration of metal-organic frameworks (MOFs) sorbents into a solar air conditioning system. Because of MOF properties, this integration allows for a thermally driven cycle without requiring a non-renewable energy input.

This thesis is comprised of six chapters geared towards assisting in the determination of the most efficient and effective means of incorporation of MOFs into AC systems. Primarily by conducting an extensive literature review, the third chapter discusses Metal Organic Frameworks in depth for determining the most suitable candidates for this research project. Specific needs for the system are examined with different MOFs that meet the criteria considered. In chapter four, feasibility of integrating MOFs into a membrane through sorption measurements is tested for candidate MOF CAU-10. Chapter five is centered around modeling a MOF-assisted indirect evaporative cooler using *EES: Engineering Equation Solver*. Modeling outputs give a preliminary understanding of the cooling process and its effect on temperature.

Together, these chapters move toward showing the feasibility of operation and its applicability to the field of renewable AC. The study of MOF attributes in Chapter 3 focused on Relative Humidity (RH) at which the MOFs demonstrated a steep water uptake, water adsorption capacity, temperatures for MOF regeneration, long term stability, and cost to synthesize and fabricate. These investigations showed $\text{Co}_2\text{Cl}_2(\text{BTDD})$, MIL-101, MIL-100(M), MOF-841, and CAU-10 to be the most promising applicants. Through sorption measurements of MOF material CAU-10 its isotherm demonstrated a capacity at the adsorption step below $0.30 \text{ g}_{\text{H}_2\text{O}}/\text{g}_{\text{MOF}}$ but a maximum capacity over $0.5 \text{ g}_{\text{H}_2\text{O}}/\text{g}_{\text{MOF}}$. The *EES* model results showed 80-90% of recycled air provides a supply temperature necessary for indoor cooling below 21°C . Chapter six summarizes all results and gives recommendations focused on thermodynamic optimization.

Acknowledgments

I would like to acknowledge and sincerely thank my advisor Dr. Jordan D. Clark for his guidance and for being a continuous source of knowledge throughout this research project. Beginning a yearlong research project requires a commitment to each other and trust in their abilities. The lessons I have learned in the academic and professional realms will be carried with me forever and I genuinely appreciate the opportunity.

I would also like to thank Saba Zakeri Shahvari and Vahid Ahmadi for being points of contact while using software programs and the literature reviews I conducted.

Table of Contents

Abstract.....	iii
Acknowledgments	iv
List of Tables	vi
List of Figures.....	vii
Chapter 1. Introduction.....	1
1.1 Background on Air Conditioning Systems.....	2
1.2 Improved Cooling Methods.....	2
1.3 Integration of Metal Organic Framework (MOF)	5
Chapter 2. Scope and Objectives.....	7
2.1 Project Scope & Objectives.....	7
Chapter 3. Identification of Candidate MOFs	8
3.1 Literature Review	8
3.2 Elite MOF Candidates	11
3.3 MOF Conclusions.....	13
Chapter 4. MOF Adsorption Tests	14
4.1 Objectives & Review of CAU-10.....	14
4.2 Experimental Methodology	14
4.3 Results & Isotherm Modeling	16
Chapter 5. System Modeling	19
5.1 System Description.....	19
5.2 Governing System of Equations.....	20
5.3 EES Results	22
Chapter 6. Conclusions and Recommendations	24
6.1 Summary and Conclusions	24
6.2 Recommendations for Future Work	24
Appendix A. EES Code.....	25
Bibliography	26

List of Tables

Table 1: Notable MOF candidates.....	11
Table 2: CAU-10 Sorption Measurements	17
Table 3: Parametric table X% vs. T2.....	22

List of Figures

Figure 1: Basic arrangement of a simple vapor-compression cooling cycle [5]	2
Figure 2: Direct Evaporative Cooler	3
Figure 3: Psychometric chart of evaporative cooling in different climates.....	3
Figure 4: Indirect evaporative cooling system	4
Figure 5: Psychometric chart utilizing desiccants and indirect cooling	5
Figure 6: MOF AC conceptual design.....	6
Figure 7: Classifications of Isotherm types [11]	9
Figure 8: Adsorption and Desorption Schematic	10
Figure 9: Espec chamber used for climate control	15
Figure 10: Ohaus Adventurer precision balance	15
Figure 11: Temperature and Humidity settings for Espec chamber	15
Figure 12: MOF integrated membrane and structure	15
Figure 13: CAU-10 Adsorption Isotherms from Testing	18
Figure 14: Indirect Evaporative Heat Exchanger “X%” recycled air.....	19
Figure 15: Indirect Cooler with Equation Positions	20
Figure 16: Plot T2 vs. X%	23

Chapter 1. Introduction

In the United States air conditioning (AC) systems are used in over 75% of homes and account for over 5% of all the electricity produced in the U.S. [1] Indoor air conditioning is now an integral part of life and commonly operates using a process known as vapor-compression cooling represented in Figure 1 below. The demand for these systems has continued to increase in recent decades as technological advancements are allowing society to be more modern and comfort driven. Today, challenges arise with altering these common practices of cooling to focus on energy efficiency and sustainability. This is due several reasons, described below. The need for a low energy and renewable solution while still encompassing a cooling cycle is imperative.

One reason air conditioning must be made more sustainable is that, refrigerants released into the atmosphere from pressurized air conditioning systems are hundreds of times more effective as greenhouse gases than carbon dioxide. However, the compounds are needed for current technology to operate because of their thermodynamic properties. When comparing common refrigerants used today such as R410A, its global warming potential is over 2000 times that of CO₂ [2].

Secondly, peak power demand is a contributing factor for over-taxing electric grids. Typically, AC demand is highest when electricity is also most needed for other purposes. Power stations must be equipped for peak demand hours meaning only a fraction of peak capacity is used other times of the year, making them very costly and inefficient. For example, countless employees leave work every day around 5:00 PM. Upon arrival at home, the majority turn on lights, cook, and use their AC unit in the summer. In the hottest parts of the U.S., AC alone accounts for over 70% of residential demand during these peak hours [3].

This national concern of global warming calls for a solution that will not only benefit the U.S. but will also provide economical and efficient energy to undeveloped countries throughout the world. Focusing on renewable energy, such as solar, would beneficially impact countries like India who receive high sun intensity throughout the year but do not have the resources to provide sufficient or clean electrical power. Developing countries expect increase in AC demand from population growth, urbanization, and income growth. This anticipated progression is estimated to raise global temperatures 0.5°C by the end of the century [4]. With fossil fuels having unsustainable influences and aging electric grids overstressed to match increasing electricity demand, the solution to a potential shortage can be found in renewable sources.

1.1 Background on Air Conditioning Systems

The vapor-compression cooling cycle consists of an evaporator, condenser, compressor, and expansion valve. Each of the four main parts of the cycle work together to lower indoor air temperatures by changing the phase and pressure of a refrigerant in a particular sequence. The compressor first pressurizes the refrigerant. As the refrigerant's gas molecules experience an increase in pressure, the temperature increases with it and it becomes a superheated gas. Energy is then rejected from the hot gas flowing through the condenser, acting as a heat exchanger, to reduce the temperature until it returns to liquid phase, after which pressure is reduced. The next critical step is through the evaporator coils in a liquid phase. The low temperature refrigerant is flowing through the coils and absorbs sensible heat from the surrounding air to cool it through evaporation. This is known as conditioned air, which is circulated into a room using a fan for comfort cooling.

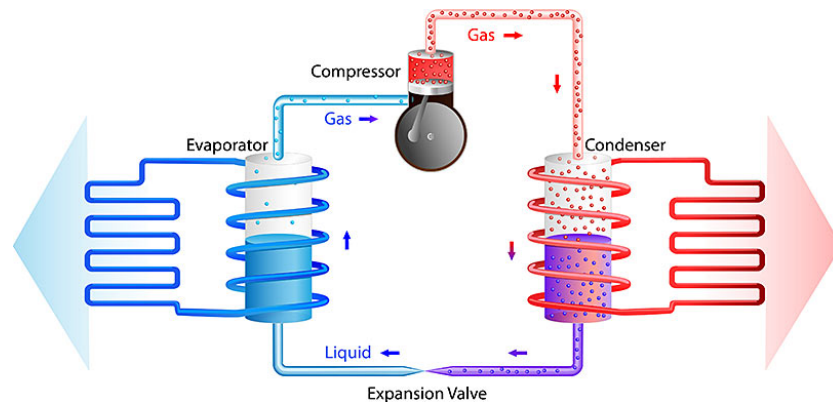


Figure 1: Basic arrangement of a simple vapor-compression cooling cycle [5]

1.2 Improved Cooling Methods

In order to improve the cooling process, more sustainable inventions of air conditioning have been created. For example, evaporative coolers, demonstrated in Figure 2, use significantly less energy and do not rely on carbon-based refrigerants. To operate, this system runs hot, dry outside air over a wet evaporative pad pulling from a continuous water supply. The water evaporates and absorbs the sensible heat causing outside air to increase in relative humidity but decrease in dry bulb temperature [6].

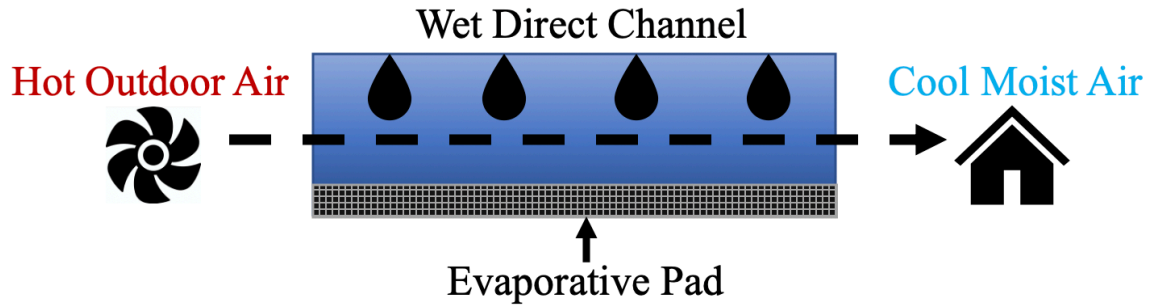
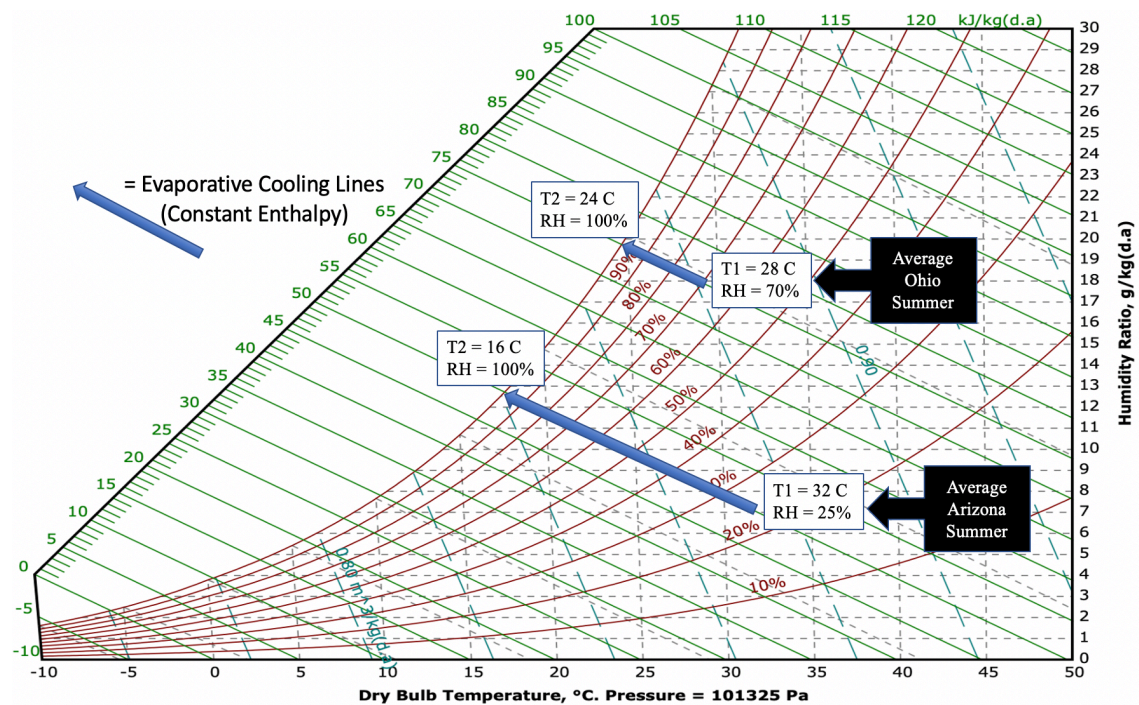


Figure 2: Direct Evaporative Cooler

However, a limitation to these coolers exists because they can only be used in dry climates such as Arizona where the outdoor air is dry enough for a significant temperature drop before saturated. Shown in Figure 3, a psychrometric chart explains how climate conditions dictate cooling abilities. Indirect cooling is a constant enthalpy process, so, for the air to reach cool enough temperatures it must be at a low relative humidity and humidity ratio. Following constant enthalpy lines on the chart, it shows the limited cooling effect on an average summer day in Ohio. In the majority of cities, sufficient cooling isn't possible unless moisture is removed from the air.



Another generation of AC technology uses a similar process but improves it by including *indirect* evaporative cooling for chilling air in a broader range of climates [6]. The indirect evaporative cooler reduces dry bulb temperatures without increasing

humidity ratios. An indirect evaporator utilizes two separate channels with airstreams flowing on both sides of a center wall shown in Figure 4 below. The top airstream flows with hot outdoor air and the second lower stream is from recycled exhausted air. The second stream is a working wet channel using the same direct evaporative process as before absorbing latent heat. By constantly evaporating, the wet surface transfers heat out of the dry channel and sensibly cools the top airstream. Cool dry air is circulated into the building while the entire process provides low-energy air conditioning.

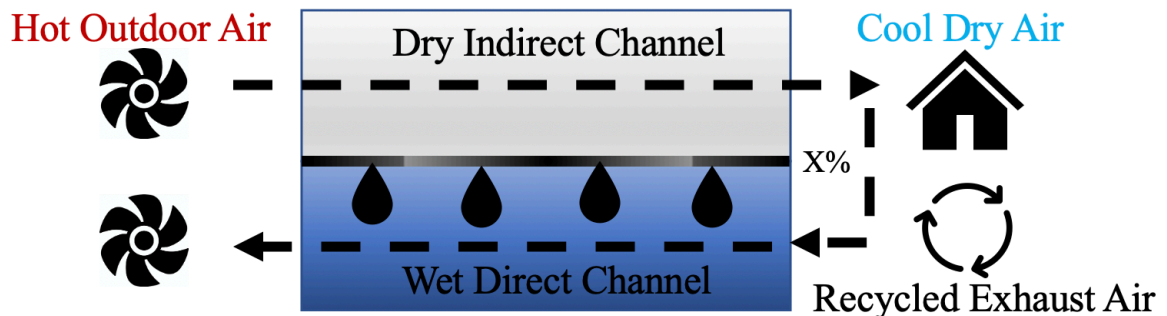


Figure 4: Indirect evaporative cooling system

Although this technology is more efficient it still suffered from climate limitations, leading to the introduction of desiccant dehumidifiers [7]. Desiccants use adsorption or absorption to remove moisture out of the intake air before it flows through the cooler. Figure 5 illustrates the individual and overall processes on a psychrometric chart. T1 represents average ambient conditions in Ohio. Following the arrow reaching T2 again shows the limitation of direct evaporative cooling in humid climates. The gray arrow represents unaccompanied indirect evaporative cooling while the green arrow shows the constant enthalpy process of a desiccant drying air. However, introducing a desiccant to dry the intake air while simultaneously cooling is shown by the red arrow angled down towards T2d. The “d” stands for dried air with significantly reduced moisture content. The dried air now has potential for dropping to a temperature cool enough for indoors. T3i, with “i” representing indirect evaporation, is limited by how cool the air in the lower direct channel can become based on the amount of recycled exhaust air.

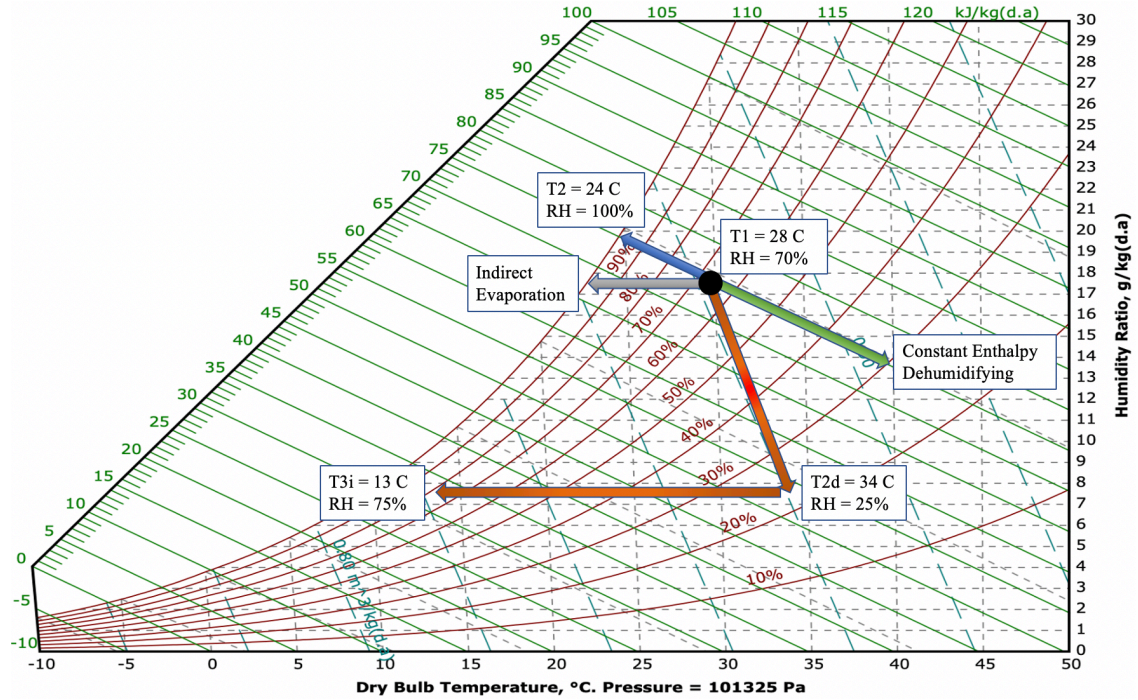


Figure 5: Psychrometric chart utilizing desiccants and indirect cooling

One shortcoming of these dehumidifiers is saturation and needing to release the adsorbed water to continue drying air. This is done with heat and evaporation but not until they reach temperatures above 120 °C for sufficient regeneration [8], when using traditional desiccants. Temperatures that high require an external non-renewable energy supply, which then contributes to green-house gas emissions. Fossil fuel boilers are an example of thermal heaters sufficient to release the adsorbed water.

1.3 Integration of Metal Organic Framework (MOF)

Using the same cyclic process with an indirect evaporative cooler and air-drying component a new solution has been proposed. Specifically, the sustainable integration of metal-organic frameworks (MOFs) in a solar AC system. MOFs functionally are a solid metal atom uses adsorption to create a thin surrounding film of liquid molecules [8]. They are favored in this research because of their high moisture uptake capacity and the low temperatures at which they can be regenerated. Combining these characteristics, MOFs are an ideal candidate for applications in clean energy.

Unlike previous research attempts in this field, MOFs are able to be engineered and regenerate at achievable solar heater temperatures around 75 – 90 °C. Their ability to release adsorbed moisture at low temperatures, distinct from previously used hygroscopic material, is key in making MOFs a potentially transformative component of open-cycle adsorption-based air conditioners. This allows for the possibility of a cycle being driven entirely by low-quality heat such as that derived from a solar thermal water heater. This could eliminate the need for non-renewable energy inputs, make air conditioning more

energy-efficient and dramatically reduce GHG emissions. The Figure below conceptually represents the model and functions along with a general psychrometric chart to explain trends.

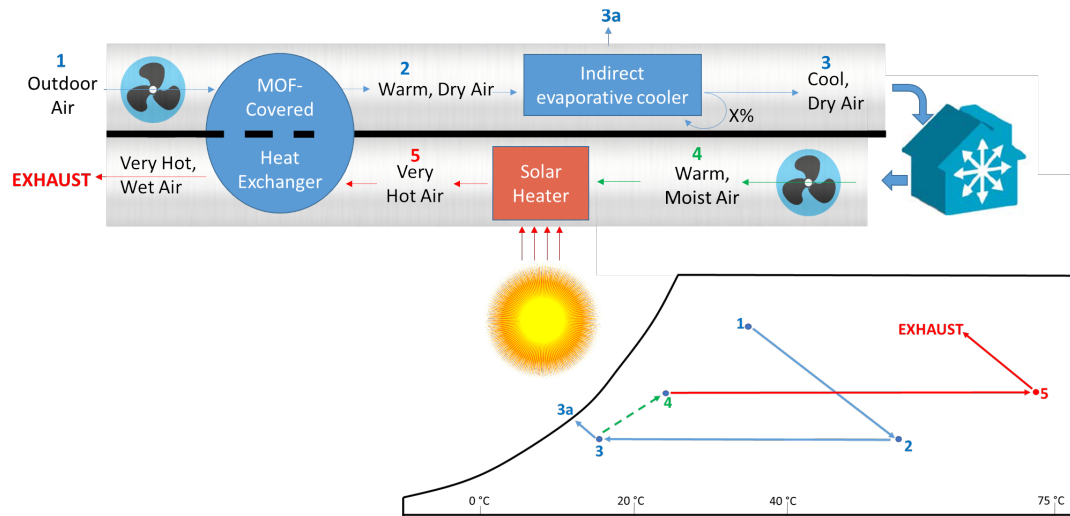


Figure 6: MOF AC conceptual design

Beginning at Stage 1, outdoor air is passed over an MOF-covered heat exchanger using a fan. The MOF, because of its adsorption properties, attracts the water molecules from the humid air so they adhere to its surface. By Stage 2, the air is dry and advances through an indirect evaporative cooler to reduce its temperature without accumulating any moisture. An optimized percentage of the cooled air, X, is recycled and used to further cool the intake air before it is exhausted at 3a. At Stage 3, conditioned dry, comfortable air is sent to the building. At Stage 4 the air has been affected by indoor environments raising its temperature and humidity. Air is circulated out of the building passing through a solar thermal heater. Using renewable energy from the sun, the air will reach a temperature around 70 °C+ before it once again passes through the MOF-covered heat exchanger. The significant property mentioned beforehand is the MOF's ability to regenerate at temperatures achievable by solar technology. So, the hot air causes the MOF to release the adhered water. This leads to the final stage where the air is exhausted both hot and at nearly 100% relative humidity.

Chapter 2. Scope and Objectives

2.1 Project Scope & Objectives

This project was completed in three distinct phases:

1. In Phase One, the main focus of this research, we conducted a literature review to help select the most suitable candidates based on factors such as water adsorption capacity, particle size, regeneration temperature, and economic viability for the project.
2. In Phase Two, we integrated MOFs into a membrane and measures their sorption property using temperature and humidity-controlled equipment. This facilitated measurement of adsorption capabilities and determined if MOF properties are retained on the integrated membrane.
3. In Phase Three we used the *EES* software to model a system that integrates the membranes and conducted a very simple thermodynamic analysis using energy and mass balance equations. Once assumptions and conditions were set, we determined an optimal percentage of recycled air for ideal system control and air temperatures.

Chapter 3. Identification of Candidate MOFs

3.1 Literature Review

In recent years, studies and synthesis of Metal Organic Frameworks have grown significantly. Realizing their unique abilities has led to their integration in many different applications. They are exceptional with their uniform porous structures, tunable porosity, flexible geometry, and extensive varieties all proving advantageous. Their structure can also be adjusted to attract particular molecules for fluid storage [9]. Corresponding to Figure 6 for this research with a tunable attraction to H₂O in adsorption-driven heat exchangers.

For this research and evaluation of the best MOF candidates, we considered over 20 materials and analyzed their properties to determine the most suitable options for the renewable AC system. Each candidate was studied through an in-depth literature review looking for MOFs with a capacity above 0.40 g_{H₂O}/g_{MOF} and a step water uptake at a relative humidity of less than 40%. The regeneration temperature must be below 100 °C and have a promising stability for commercial use. Lastly, economical choices must be taken into account for testing and commercial applications.

Location of Step:

An important MOFs property is the location of the adsorption isotherm “step”. The step refers to the relative humidity at which the adsorbed moisture (grams of H₂O held per gram of MOF) on the MOF experiences a steep increase. This sudden step is what defines the system and signifies what relative humidity causes H₂O to quickly adhere to its surface and condense in pores. Pore hydrophilicity must be sufficient for water nucleation and pore filling below 40% RH for most commercial applications [10]. A higher step location may limit adsorption potential in certain climates and require too much energy to achieve.

Isotherm steps are categorized by shape, which determines the adsorption and desorption processes. Figure 7 displays six isotherm categories based on their shape comparing amount adsorbed versus relative pressure or humidity. In this research, an “S” shaped isotherm, type V, is ideal which is based on microporous structure interactions. Type V is desired because it has the most abrupt step of H₂O adsorbed within a small range of relative humidity values for better system control.

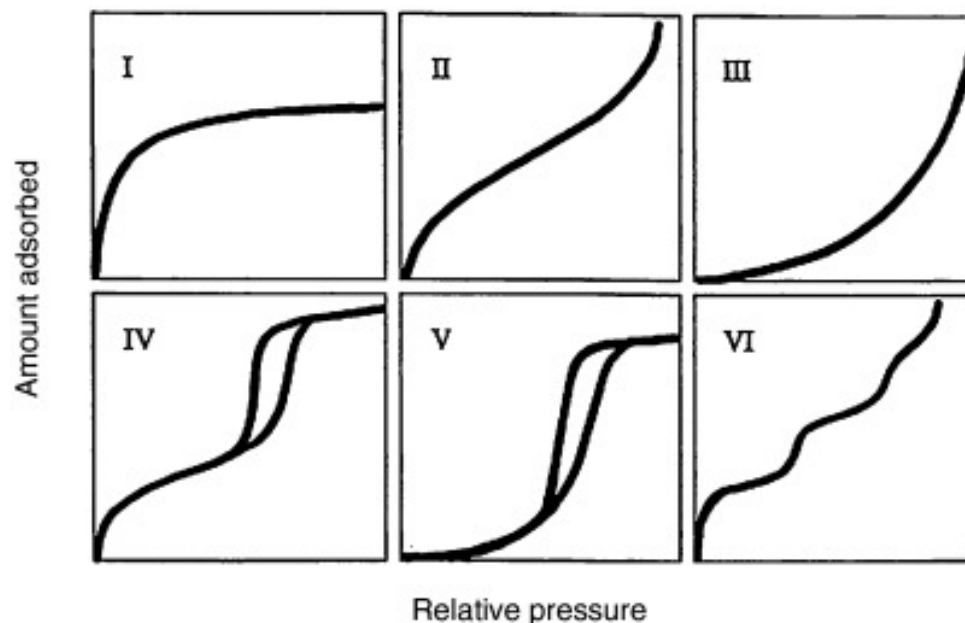


Figure 7: Classifications of Isotherm types [11]

Capacity:

The capacity of a MOF is how much H_2O it can adsorb. Adsorption properties are described by the isotherm shape and occur because the MOF's engineered structure has an affinity for water onto its surface. The greater the attraction and surface area, the higher uptake capacity possible. Higher H_2O capture, above $0.40 \text{ g}_{H_2O}/\text{g}_{MOF}$, allows for more humidity control over the ambient intake air [12]. Also making the design efficient with the amount of MOF needed for proper dehumidifying in humid climates.

Regeneration Temperature:

Contrarily, this attraction causes MOFs to become completely saturated and need desorption, or to release the H_2O molecules. Figure 8 demonstrates the surface of a MOF. As %RH increases, layers of molecules form by adsorbing to the surface but a decrease in pressure allows for desorption. The greater attraction between the molecules and MOF surface means a higher temperature needed for desorption to occur. Regeneration for the MOF is noted as the temperature required to release all adsorbed H_2O ; comparable to drying a wet sponge and needed to continue dehumidifying air in real-world applications. Efficient regeneration is essential for choosing a good candidate. Lower temperatures, which is correlated to low energy, is important for using solar thermal heaters who are only capable of providing temperatures below 100°C .

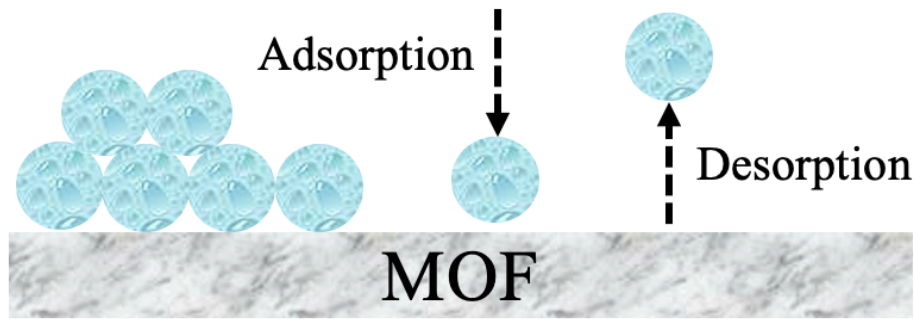


Figure 8: Adsorption and Desorption Schematic

Stability:

Lastly, an important factor is how stable the MOF is, which has been a major inhibitor of commercial technologies being produced. Stability is quantified by the number of times the MOF experiences adsorption-desorption cycles without permanently degrading sorption abilities. It is important because with long-term consistency comes opportunity for more cyclic applications. When considering applications, MOFs need to withstand H₂O cycling in both heat and pressure intensive environments. Usually measured by loss of capacity, cycling MOFs is an energy-intensive process that can lead to crystallinity destruction. Once the crystal structure changes, bonding locations aren't as easily accessible by water molecules [12]. Even materials such as MOF-5 are thermally stable to 300 °C, but not water stable and cannot survive in humid air, diminishing usefulness in AC applications [13].

As can be seen in Table 1, among the thousands of MOF materials, a small number meet the desired criteria. But the uniqueness of MOFs stands out particularly in certain performers. For example, Cr-SOC-MOF-1, a MOF synthesized with Chromium as the metal ion. It has one of the highest maximum capacity's reaching 2 grams of water vapor uptake per gram of material. And it does so at a RH of 70% [12]. Another example of a unique MOF is CPO-27(Ni). This material demonstrates a type I isotherm but reaches over 75% of its 0.47 g_{H2O}/g_{MOF} capacity before it crosses 5% RH [14]. Its microporous structure is very attractive for water molecules and useful in environments with dry climates. Some materials exhibit great stability like MOF-303 and after 150 cycles no degradation of the compound was shown. This material, however, has an H₂O step uptake less than 0.30 g_{H2O}/g_{MOF} hurting its potential for commercial manufacturing [15]. The following table summarizes findings from the literature review and described in the next section.

Table 1: Notable MOF candidates

MOF	Capacity @ Step	RH% @ Step	Max Capacity	Adsorption Temp	Regeneration Temp	Stable Cycles	Isotherm Type
MIL-101	0.90	40	1.01	40	90	40	IV
MOF-801	0.21	10	0.4	30	80-85	5	IV
CAU-10-H	0.20	20	0.26	25	70	10000	V
MIL-100 (Fe)	0.70	40	0.75	25	50-90	40	IV
MIL-100 (Al)	0.40	40	0.5	25	50-90	40	IV
NH ₂ -MIL- 125	0.40	10-20	0.45	30	75	10	V
UiO-66	0.30	25-35	0.36	20	80	10	I
CPO- 27(Ni)	0.40	5	0.47	25	90	10	I
Aluminum Fumarate	0.35	20-30	0.53	25	50-70	10	IV
MIL-160	0.35	8-20	0.40	25	90	-	V
MOF-303	0.30	15-30	0.48	15	65	150	IV
MFU-4l	1.01	60-70	1.05	25	-	-	IV
MOF-841	0.40	25	.50	25	45*	5	V
Co ₂ Cl ₂ (BT DD)	0.82	45	0.97	25	45*	30	IV
Cr-SOC- MOF-1	1.95	70	2.00	25	25*	100	V

*Indicates Desorption Temp instead of Regeneration

3.2 Elite MOF Candidates

Despite uniqueness a number of MOFs stood out as elite candidates above the rest. For example, MIL-101, a chromium-based material, has the potential to sufficiently perform in the AC system with a notable 0.90 g_{H₂O}/g_{MOF} uptake by 40% relative humidity. MIL-101 reaches a maximum capacity at 1.01 g_{H₂O}/g_{MOF} before regenerating at less than 90 °C [16]. The complete isotherm takes a type IV shape and after 40 test cycles, 96.8% of water uptake capacity is maintained deeming this a highly stable substance for an adsorption heat-exchanger compared to other MOFs. However, long term stability in commercial applications is still in question.

Co₂Cl₂(BTDD) is created with chlorine (Cl) and cobalt (Co) as its metal cation. This MOF demonstrates a type IV isotherm with its step beginning around 30% RH. The step is nearly vertical reaching 0.82 g_{H₂O}/g_{MOF} and in addition there is minimal hysteresis from adsorption to desorption. This MOF has a maximum capacity of 0.97 g_{H₂O}/g_{MOF} and experiences desorption at 45 °C. A low desorption temperature easily achievable by a solar heater and high capacity make this MOF among the most promising materials.

Although these features meet the desired criteria, 6% loss of capacity was shown after 30 cycles again bringing up potential long-term issues with commercial technologies [18]. Cobalt is also over 30 times more expensive than aluminum, taxing on large-scale production [17].

As mentioned, a benefit of MOFs is their extensive varieties and infinite tunability. MIL-100(M) is an example of synthesizing materials to change its properties. (M) represents elements including iron (Fe) and aluminum (Al) [14]. With different bonding metal ions changes its properties and cost. Aluminum already being a low-cost material at \$1.91/kg is still over 20 times more expensive than iron at \$0.08/kg [17]. The change in material has an effect on the isotherms and overall capacity. Although the type IV shape is consistent with both, MIL-100(Al) shows 30% less hysteresis on its isotherm than that its counterpart. MIL-100(Fe) reaches 0.70 $\text{g}_{\text{H}_2\text{O}}/\text{g}_{\text{MOF}}$ at 40% RH before gradually reaching a maximum capacity of 0.75 $\text{g}_{\text{H}_2\text{O}}/\text{g}_{\text{MOF}}$. MIL-100(Al) adsorbed 0.40 $\text{g}_{\text{H}_2\text{O}}/\text{g}_{\text{MOF}}$ by 40% RH and steadily increases until its max capacity of only 0.50 $\text{g}_{\text{H}_2\text{O}}/\text{g}_{\text{MOF}}$. Hydrothermal stability is impressive for both materials noting no damage to crystallinity during testing. But after 40 cycles around 6.5% reduced water capacities were shown becoming less hydrophilic and highlighting an area of future research with stability measurements [19].

UiO-66 is a zirconium-based compound. Zirconium MOFs have proven useful in products for adsorbing moisture from desert air during humid nights in order to desorb it for drinkable water during the hot day. Aluminum is cheaper to scale for manufacturing but not as effective because of zirconium's affinity for oxygen [20]. In terms of abilities UiO-66 has a maximum capacity of 0.36 $\text{g}_{\text{H}_2\text{O}}/\text{g}_{\text{MOF}}$ and regenerates at 80 °C. The isotherm begins rising at 0% RH but abruptly spikes between 25%-35% reaching 0.30 $\text{g}_{\text{H}_2\text{O}}/\text{g}_{\text{MOF}}$. This material's capacity hasn't shown degradation after 10 cycles, but the isotherms occur at lower RH in comparison to the first sorption cycle. Meaning this material is hydrophilic in nature [21]. Although the stability in this MOF is promising its capacity is limiting for commercial use.

MOF-841 is another example of a zirconium-based product but has improved stability and capacity. With only slight adsorption until 25% RH, this MOF has a near vertical step reaching over 0.40 $\text{g}_{\text{H}_2\text{O}}/\text{g}_{\text{MOF}}$ and plateauing for a slight incline to maximum capacity just below 0.50 $\text{g}_{\text{H}_2\text{O}}/\text{g}_{\text{MOF}}$. Such a steep incline represents H_2O quickly condensing in the materials pores creating a type V isotherm. Minimal hysteresis is displayed when desorption occurs at 45 °C. Unlike the majority of MOFs, capacity is constant even after 5 adsorption-desorption sequences [22]. With its uptake greater than 40 weight percent at 30% RH it's one of the highest for a porous solid but this weight percentage is nearly doubled by $\text{Co}_2\text{Cl}_2(\text{BTDD})$ [10]. This material's clear, abrupt step allows for easier model predictions with AC climate control and proving to be one of the best materials for future use if framework stability against capillary forces can be confirmed.

Aluminum Fumarate has been recognized for hydrothermal stability and operational water uptake over 0.50 $\text{g}_{\text{H}_2\text{O}}/\text{g}_{\text{MOF}}$. Regenerating between 55-70 °C shows an ideal temperature [23]. This MOFs isotherm takes a type IV shape with a step capacity increase between 20-30% RH reaching 0.35 $\text{g}_{\text{H}_2\text{O}}/\text{g}_{\text{MOF}}$. Limited adsorption before 20%

RH is due to hydrophobicity of the organic linker but hydrophilic inner aluminum pores [22]. Even at different adsorption temperatures this material shows consistent uptake. Stability has been tested for ten cycles showing a slight decrease with each of the first four cycles but then consistent values above 0.45 g_{H2O}/g_{MOF} afterwards when equilibrium was reached. This equilibrium stability opens up potential for long term commercial applications, but its capacity doesn't reach AC requirements.

3.3 MOF Conclusions

The uniqueness of MOFs becomes apparent when describing their characteristics and diverse abilities. But one conclusion that holds true for the majority of high performers is lack of stability. Several elite candidates showed a loss of H₂O capacity after a number of adsorption-desorption cycles and will need further testing before commercial applications can be designed around them. However, determining g_{H2O}/g_{MOF} capacities and correlating relative humidity, general material expense, and regeneration temperatures allows for modeling to begin as MOF testing resumes. These numbers are essential to prove the economic and environmental impacts in a range of effective environments. MIL-101, Co₂Cl₂(BTDD), MOF-841, and MIL-100(M) show the greatest potential in solar air conditioning.

Chapter 4. MOF Adsorption Tests

4.1 Objectives & Review of CAU-10

Understanding the properties studied in literature, testing and measurements of a MOF material known as CAU-10 were performed. CAU-10 is an economically practical material and more easily synthesized using aluminum as its metal ion. Among its notable features is CAU-10's unparalleled stability retaining capacity even after 10,000 adsorption-desorption cycles and a 70 °C regeneration temperature [18]. Both abilities prove its long-term usefulness in this research and for achievable solar thermal heater temperatures. This motivated the testing of feasibly integrating the MOF into a membrane through sorption measurements. When integrated, different temperatures and humidity's were cycled to determine if MOF properties were still retained once in the membrane. Other objectives were to understand if the isotherm is temperature dependent and how the material reacts under cycling.

4.2 Experimental Methodology

Once the CAU-10 material was synthesized, characterized and integrated on a membrane (by collaborators in the Departments of Chemistry; and Chemical and Biomolecular Engineering), adsorption tests were performed on the MOF using an environmental chamber. The chamber is set to a specified temperature and humidity level to simulate real-world climate conditions. In order to create a complete isotherm, the temperature for these tests was held constant at 35 °C, 45 °C, and 65 °C while humidity increased at intervals between 10% and 90% RH for each temperature. Initially, the weight at ambient conditions outside the chamber was recorded. Then, the MOF was placed inside the chamber after setting temperature and humidity values. An adequate amount of time was given to reach equilibrium before recording weight measurements at each increasing humidity.

Below is the instrumentation used in the experiments. Figure 9 is the Espec BTL-433 benchtop temperature and humidity test chamber with a 4 cubic foot volume. The chamber is used for simulating different conditions set by the controller on the outside of the chamber with examples in Figure 11. Conditions were set by the controller but measured more accurately by a Fisherbrand digital hygrometer/thermometer inside the chamber. With a temperature range -40 to 104 °C its digital display accuracy is $\pm 0.4^{\circ}\text{C}$ and $\pm 1.5\%$ RH with 0.1°C resolution. The chambers operating temperature ranges between -20 °C to 180 °C and humidity ranges 10 to 95 % RH. Typically, it uses 0.5 gallons of water for humidity control per day, which was supplied manually from a water tank in these tests.

After CAU-10 had reached equilibrium, it was quickly transferred onto the Adventurer precision AX422/E balance in Figure 10. The scale has a maximum capacity of 420 g and readability to 0.01 grams with results shown on its touch display. Powered by an AC adapter, its functional working environment is between 10-30 °C and up to

80% RH. Figure 12 show the MOF-integrated membrane sheets combined on the provisional structure. The structure was wholly placed in the chamber and weighed with the MOF for accurate measurements.



Figure 9: Espec chamber used for climate control

Figure 10: Ohaus Adventurer precision balance



Figure 11: Temperature and Humidity settings for Espec chamber



Figure 12: MOF integrated membrane and structure

4.3 Results & Isotherm Modeling

Using these instruments and testing procedures, measurements were recorded, showing Table 2. This data is plotted on Figure 13, which indicates CAU-10 has a steep uptake around 20% RH and a type V isotherm shape. This MOF has a low capacity under $0.30 \text{ g}_{\text{H}_2\text{O}}/\text{g}_{\text{MOF}}$ at its step but reaches an average maximum capacity just above $0.50 \text{ g}_{\text{H}_2\text{O}}/\text{g}_{\text{MOF}}$ at 90% RH. The plot includes three distinct isotherms, which are averages of all the tests completed at each temperature. Each test measures MOF uptake at the corresponding RH% and the change in H_2O mass is plotted. Error bars are included to graphically represent uncertainty in the data between tests.

At lower isotherm temperatures, the MOF has a more abrupt step occurring at a lower relative humidity. For 35°C the step begins to plateau at 20% RH while at 45°C isotherm step starts plateauing at 30% RH. The average step uptake at 45°C is only $0.015 \text{ g}_{\text{H}_2\text{O}}/\text{g}_{\text{MOF}}$ higher despite the shift in step. The 65°C isotherm closely mimics the 45°C trend but its step and max capacity average another $0.015 \text{ g}_{\text{H}_2\text{O}}/\text{g}_{\text{MOF}}$ higher. Concluding, MOF properties are qualitatively still retained once the MOF is integrated into a membrane, and the step capacity is not drastically influenced by temperature.

These are the first sets of experiments, which were cut short by COVID-19 during the 2020 epidemic. Given sufficient time, each test would have been repeated and others performed to determine repeatability for quantifying uncertainty. Other limitations include weight measurements techniques. In this case, at each temperature and %RH, the MOF structure was taken out of the test chamber to place on the scale. In that brief transition time under five seconds, the ambient conditions can quickly affect the MOF uptake and introduce a potential source of error. To solve this problem, in future experiments a small opening will be drilled into the top of the chamber and sealed with a digital hanging balance inside. This will allow the MOF to be measured at equilibrium without removing it from the chamber.

Table 2: CAU-10 Sorption Measurements

Temperature (°C)	Relative Humidity	Test 1 Mass (g)	Test 1 Δ Mass	Test 2 Mass (g)	Test 2 Δ Mass	Test 3 Mass (g)	Test 3 Δ Mass
ambient	ambient	168.65	0.22	168.69	0.26	168.67	0.24
35	0.155	168.49	0.06	168.48	0.05	168.43	0
35	0.2	168.61	0.18	168.63	0.2	168.6	0.17
35	0.3	168.65	0.22	168.67	0.24	168.67	0.24
35	0.5	168.71	0.28	168.7	0.27	168.71	0.28
35	0.7	168.81	0.38	168.79	0.36	168.78	0.35
35	0.9	168.94	0.51	168.93	0.5	168.96	0.53
ambient	ambient	-	-	-	-	168.7	0.27
45	0.115	168.47	0.04	168.48	0.05	168.48	0.05
45	0.2	168.48	0.05	168.53	0.1	168.57	0.14
45	0.3	168.67	0.24	168.68	0.25	168.65	0.22
45	0.4	168.7	0.27	-	-	-	-
45	0.5	168.72	0.29	168.71	0.28	168.7	0.27
45	0.6	168.75	0.32	-	-	-	-
45	0.7	168.78	0.35	168.8	0.37	168.82	0.39
45	0.9	168.99	0.56	168.99	0.56	168.98	0.55
ambient	ambient	168.71	0.28	168.72	0.48	-	-
65	0.1	168.24	0	168.4	0	-	-
65	0.2	168.27	0.03	168.41	0.01	-	-
65	0.3	168.55	0.31	168.6	0.2	-	-
65	0.5	168.63	0.39	168.64	0.24	-	-
65	0.7	168.79	0.55	168.8	0.4	-	-
65	0.9	168.99	0.75	168.93	0.53	-	-

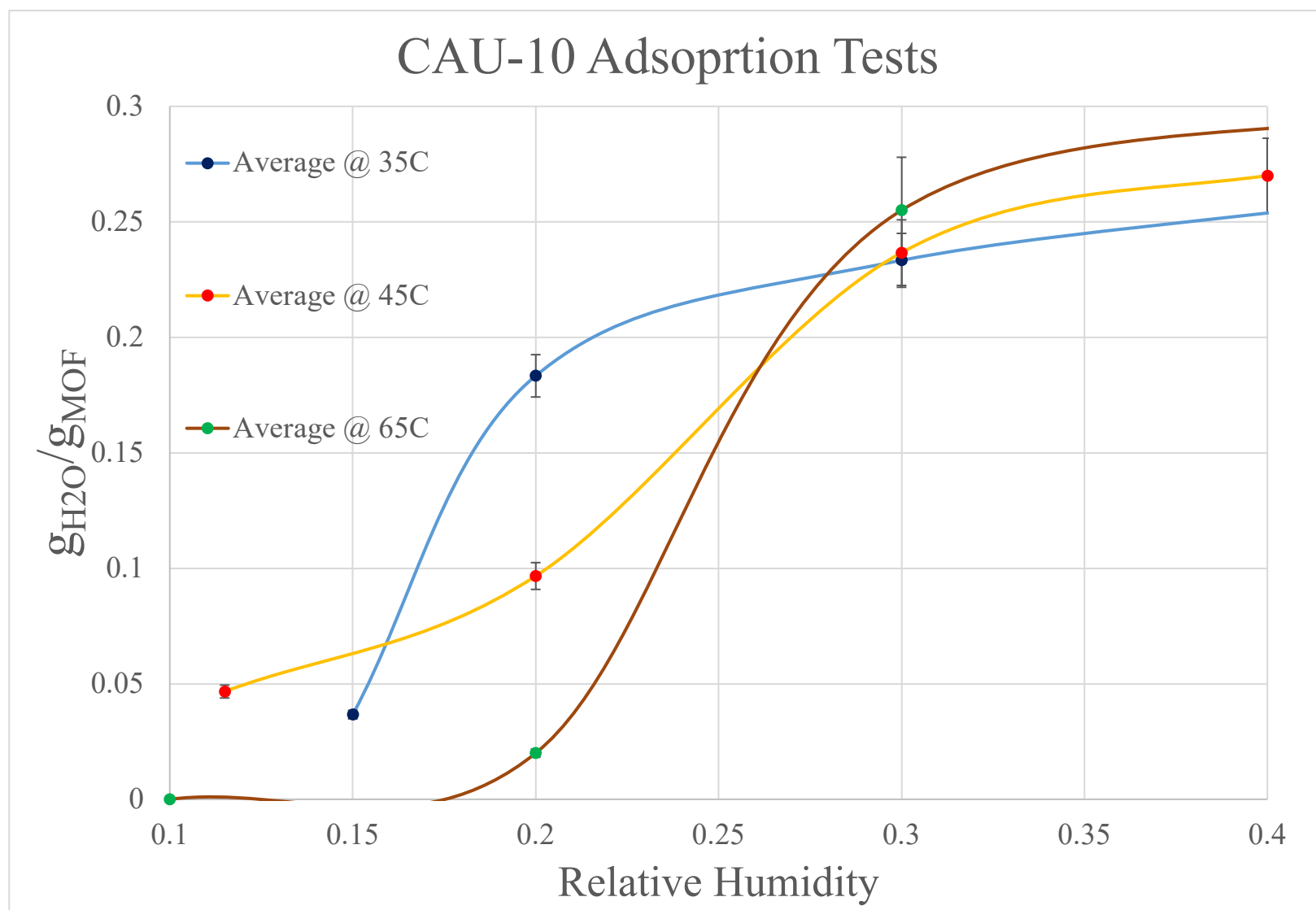


Figure 13: CAU-10 Adsorption Isotherms from Testing

Chapter 5. System Modeling

5.1 System Description

In order to begin understanding the operation of a membrane-based MOF-assisted air conditioner, we conducted initial modeling of the AC system using known air properties and representative equations. One of the key components is the aforementioned indirect evaporative cooler. As the air dried by the MOF out of the drying channel (shown at the top of Figure 14), a percentage of the dry air is recycled into the wet channel (bottom) in order to provide cooling to the supply stream (top). The supply air is what is supplied to the building at the desired temperature, typically around 12 °C. This general indirect process is shown in Figure 14, similar to Figure 4 with an emphasis on X% of recycled air.

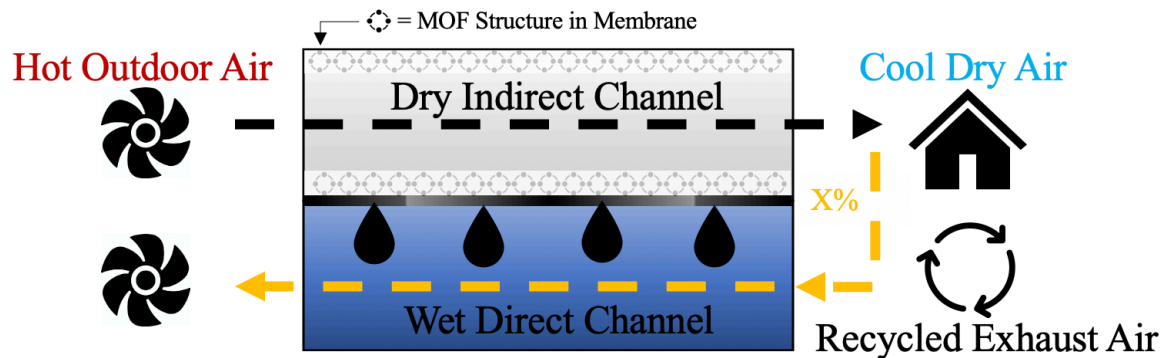


Figure 14: Indirect Evaporative Heat Exchanger “X%” recycled air

The recycled air plays a vital role in how effective the system is in reducing air temperature. X% of recycled air flows through the wet channel and performs direct evaporative cooling to attract the heat out of the dry channel without transferring moisture. A percentage too low doesn’t provide enough cooling, and too high of a percentage will make the system unnecessarily large as it decreases the amount of process air able to be supplied to the building.

To find an optimal percentage of recycled air, the *EES: Engineering Equation Solver* program was used. This software has a built-in database with thermodynamic properties and the ability to simultaneously solve equations for accurate optimization. Energy and mass balance equations were written to explain its functionality in the following section. See Appendix A for the entire program code written to represent the model.

5.2 Governing System of Equations

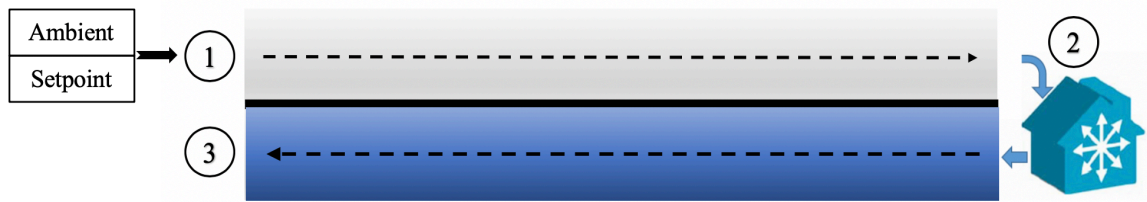


Figure 15: Indirect Cooler with Equation Positions

To begin describing the system, known states that are independent from recycling conditions were established. This includes ambient and indoor setpoint conditions, consistent pressure at sea level for all stages, and relative humidity values. Figure 15 shows where each stage is related to the cooler. At Stage 1, a mixture of ambient and setpoint conditions are flowing into the cooler. Stage 2 represents conditioned air circulated into the building. Lastly, Stage 3 is the air that has been recycled from the supply stream of the cooler after passing through the wet channel to produce the needed cooling effect.

Ambient conditions were assumed to be at 35 °C and 75% RH to simulate a hot and humid environment. Ambient air is mixed with a percentage of the indoor setpoint conditions, which would be controlled by a thermostat typically around 21 °C and 50% RH to feel comfortable inside. By Stage 2, the air has already flowed through the MOF-integrated indirect cooler to reduce the moisture content (H_2O) and temperature. Since finding the optimal temperature is the goal of the model, the only assumption at this point is humidity, which has been reduced by the MOF to 25% RH. Stage 3 is the recycled exhaust air after X% has gone through the wet, direct portion of the cooler. The air at this point is assumed to be saturated at 99% RH from the evaporating water in channel with an unconstrained temperature.

With constants properly described, *EES* has the ability to use the state variables for defining thermodynamic properties. For example, if temperature, pressure, and relative humidity are known the program can use internal psychometric principles to solve for enthalpy (h), or humidity ratios (ω), and vice versa. Once properties of the system are established, *EES* can function as a computing device and simultaneously solve equations. Substituting in each of the known values allows it to find properties that were previously undetermined. Focusing on heat transfer and moisture content in the air the indirect evaporative cooler was modeled. Below are the defined state variables, built in functions, and overall energy and mass balance equations.

EES State Variables & Built in Functions:

$$\begin{aligned}
 T_{amb} &= 35 & h_{water,in} &= h(water, T = T_1, x = 0) \\
 rh_{amb} &= 0.75 & h_{water,out} &= h(water, T = T_2, x = 0) \\
 P1 &= 101.325 & \omega_{set} &= \omega(AIRH2O, T = T_{set}, P = P1, R = rh_{set}) \\
 T_{set} &= 21 & h_{set} &= h(AIRH2O, T = T_{set}, P = P1, R = rh_{set}) \\
 rh_{set} &= 0.5 & T_1 &= T(AIRH2O, w = \omega_1, h = h_1, P = P1) \\
 P2 &= P1 & \omega_{amb} &= \omega(AIRH2O, T = T_{amb}, R = rh_{amb}, P = P1) \\
 rh_2 &= 0.25 & h_{amb} &= h(AIRH2O, T = T_{amb}, R = rh_{amb}, P = P1) \\
 P3 &= P1 & \omega_3 &= \omega(AIRH2O, T = T_3, R = rh_3, P = P3) \\
 rh_3 &= 0.99 & h_3 &= h(AIRH2O, T = T_3, R = rh_3, P = P3) \\
 & & T_3 &= T(AIRH2O, R = rh_3, w = \omega_3, P = P3) \\
 & & h_2 &= h(AIRH2O, T = T_2, R = rh_2, P = P2)
 \end{aligned}$$

Energy Balance:

$$\begin{aligned}
 \dot{m}_{total} * h_1 &= \dot{m}_{total} * h_2 * (1 - x) + \dot{m}_{total} * h_3 * x - \dot{m}_{total} * h_{water,in} * (\omega_3 - \omega_1) \\
 &\quad * x + \dot{m}_{total} * h_{water,out} * (\omega_1 - \omega_2) \\
 h_1 &= h_{amb} * x + h_{set} * (1 - x)
 \end{aligned}$$


Mass Balance:

$$\begin{aligned}
 \dot{m}_{total} * \omega_1 + \dot{m}_{water} &= \dot{m}_{total} * \omega_2 * (1 - x) + \dot{m}_{total} * \omega_3 * x + \dot{m}_{removed} \\
 \omega_2 * \dot{m}_{total} &= \omega_1 * \dot{m}_{total} - \dot{m}_{removed} \\
 \dot{m}_{water} &= (\omega_3 - \omega_2) * \dot{m}_{total} * x \\
 Y &= \frac{\dot{m}_{water}}{\dot{m}_{air}} \\
 Z &= \frac{\dot{m}_{removed}}{\dot{m}_{air}} \\
 \omega_1 &= \omega_{amb} * x + \omega_{set} * (1 - x)
 \end{aligned}$$

5.3 EES Results

After variables and units were specified the *EES* program computed the governing energy and mass balance equations. In order to understand the amount of recycled air and its effect on temperature a parametric table incrementing X between 0.01-0.99 was produced. Table 3 below shows the results. The trend follows an initial asymptote around 25 °C and then a negative, non-linear slope descending quickly after X=0.75. For a comfortable indoor temperature below 21 °C, this model determines 80%-90% of recycled air produces a sufficient cooling effect. A percentage this high might indicate the system is unnecessarily large to provide enough processed air to the building. In order to improve these results, more equation details and general assumptions may be added to the model. Different climate conditions should also be tested for ideal environments.

Table 3: Parametric table X% vs. T2

 1..10	1 x	2 T2 [C]
Run 1	0.01	25.71
Run 2	0.1189	25.55
Run 3	0.2278	25.35
Run 4	0.3367	25.08
Run 5	0.4456	24.72
Run 6	0.5544	24.2
Run 7	0.6633	23.39
Run 8	0.7722	21.96
Run 9	0.8811	18.79
Run 10	0.99	7.298

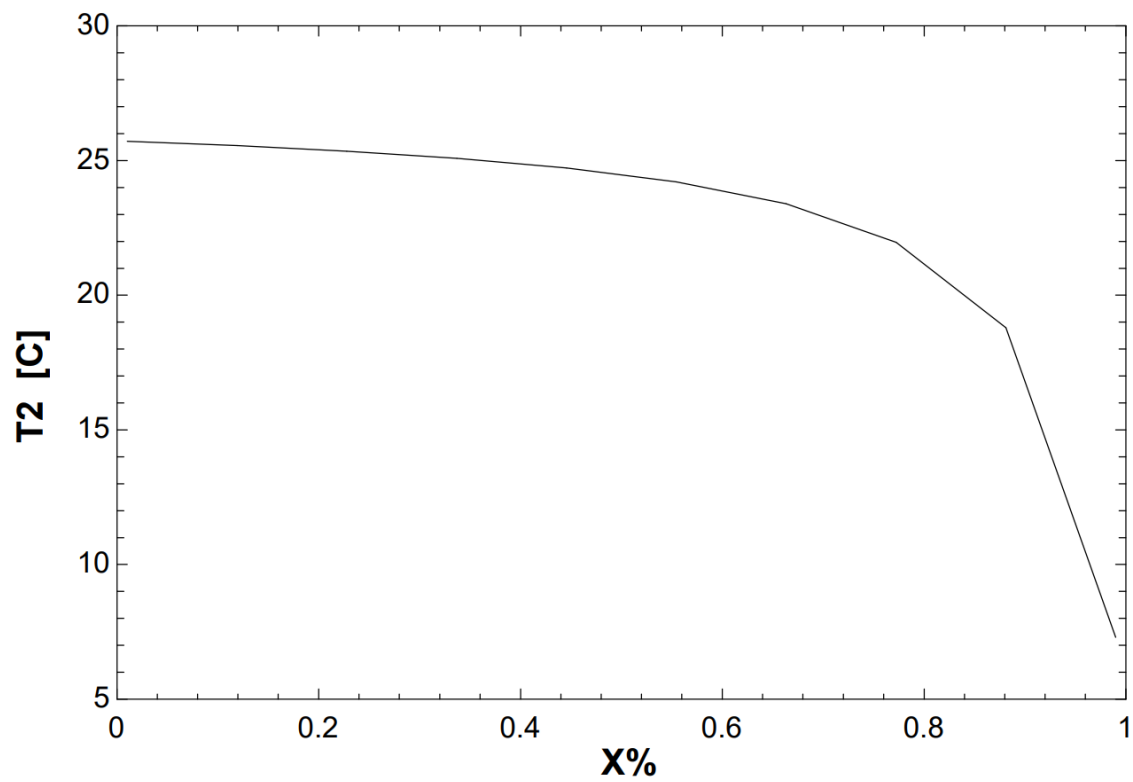


Figure 16: Plot T_2 vs. $X\%$

Chapter 6. Conclusions and Recommendations

6.1 Summary and Conclusions

The integration metal-organic frameworks (MOFs) into a solar air conditioning system remains as a potential solution to the shortcomings of past technologies trying to answer ongoing energy and GHG issues. After an in-depth literature review focused on a low Relative Humidity (RH) at which the MOF demonstrated a steep water uptake, a high capacity for gram of H₂O per gram of MOF adsorbed, low temperatures at which the MOF could be regenerated, long term stability for commercial use, and cost to synthesize and fabricate. The most ideal MOFs for commercial applications were determined to be Co₂Cl₂(BTDD), MIL-100(M), MIL-101, MOF-841, and CAU-10.

Sorption tests verified MOF-membrane feasibility. CAU-10 was tested to show how its capacity reacted under cycling and temperature effects. For 35 °C the step begins to plateau at 20% RH while at 45 °C isotherm step starts to plateau at 30% RH. The average step uptake at 45 °C is only 0.015 g_{H2O}/g_{MOF} higher despite the shift in step. The 65 °C isotherm closely mimics the 45 °C trend but its step and max capacity average 0.015 g_{H2O}/g_{MOF} higher. All isotherms at 90% RH had an uptake over 0.50 g_{H2O}/g_{MOF}. Concluding, capacity is reduced when the MOF is integrated onto the membrane, but MOF properties are still retained, and the step capacity is not drastically influenced by temperature.

Using *EES: Engineering Equation Solver* the MOF-assisted indirect evaporative cooler was modeled using energy and mass balance equations. Based on the amount of recycled air, X, the temperature to the building was optimized with X being the most optimal percentage. The temperature slope hits the desire temperature below 21 °C when X is approximately 80%-90%.

6.2 Recommendations for Future Work

As a recommendation for future work, the best MOF candidates should be tested for long-term stability. For example, the number of adsorption-desorption cycles required by an AC heat exchanger in a one-year period could be calculated to then determine each MOFs replacement lifetime. Further analysis of CAU-10's performance in the AC system should be modeled in a thermally driven heat exchanger. Lastly, using the *EES* code a more detailed analysis of the system could be accomplished with specific MOF adsorption abilities implemented into the program.

Appendix A. EES Code

```

T_amb = 35 [C]
rh_amb = .75 [-]
P1 = 101.325 [kPa]

T_set = 21 [C]
rh_set = .50 [-]

//T2 = 12 [C]
P2 = P1
rh_2 = .25 [-]

//T3 = T1
P3 = P1
rh_3 = .99 [-]

h_water_in = enthalpy(WATER, T=T3, X=0)
h_water_out = enthalpy(WATER, T=T2, X=0)

omega_set = humrat(AirH2O, T=T_set, P=P1, R=rh_set)
h_set = enthalpy(AirH2O, T=T_set, P=P1, R=rh_set)

T1 = temperature(AirH2O, W=omega_1, H=h_1, P=P1)

omega_amb = humrat(AirH2O, T=T_amb, R=rh_amb, P=P1)
h_amb = enthalpy(AirH2O, T=T_amb, R=rh_amb, P=P1)

omega_3 = humrat(AirH2O, T=T3, R=rh_3, P=P3)
h_3 = enthalpy(AirH2O, T=T3, R=rh_3, P=P3)
T3 = temperature(AirH2O, W=omega_3, R=rh_3, P=P3)

h_2 = enthalpy(AirH2O, T=T2, R=rh_2, P=P2)

omega_1 = omega_amb*(x) + omega_set*(1-x)
h_1 = (x)*h_amb + (1-x)*h_set
h_1 = (1-x)*h_2 + x*h_3 - h_water_in*(omega_3*x - omega_1) + (omega_1 - omega_2*(1-x))*h_water_out
omega_1 = -Y + (1-x)*omega_2 + x*omega_3 + Z
omega_2 = (omega_1 - Z)/(1-x)
Y = (x)*(omega_3) - (1-x)*(omega_2)

```

"Initial Temperature"
 "Relative Humidity of air"
 "Atmospheric Pressure"

"Enthalpy of water @ T_amb"
 "Enthalpy of water @ T2"

"Humidity Ratio ambient"
 "Enthalpy ambient"

"Humidity ratio @ 3"
 "h_3 > h_1"

"Enthalpy 2 -> T2"

"Equation 2"
 "Equation 3"

Bibliography

- [1] U.S. Department of Energy. (n.d.). Air Conditioning. Retrieved from <https://www.energy.gov/energysaver/home-cooling-systems/air-conditioning>
- [2] California Air Resources Board (Ed.). (n.d.). High-GWP Refrigerants. Retrieved April 20, 2020, from <https://ww2.arb.ca.gov/resources/documents/high-gwp-refrigerants>
- [3] OECD/IEA. (2018). The Future of Cooling: Opportunities for energy-efficient air conditioning. Retrieved from <https://www.oecd.org/about/publishing/TheFutureofCooling2018Corrigendumpages.pdf>
- [4] O'Grady, E., & Narsipur, S. (2018, September 18). The AC Industry Conundrum: Cooling Is Warming the Planet, but Market Failures Are Preventing the AC Industry from Innovating. Retrieved from <https://rmi.org/ac-industry-conundrum/>
- [5] Everything You Need To Know About HVAC systems. (n.d.). Retrieved from <http://twentyonecelsius.com.au/blog/everything-you-need-to-know-about-hvac-systems/>
- [6] Rezaee, V., & Houshmand, A. (2015, June 1). Feasibility Study Of Maisotsenko Indirect Evaporative Air Cooling Cycle In Iran. Retrieved from https://content.sciendo.com/view/journals/gse/61/2/article-p23.xml?lang=en&tab_body=contentReferences-69374
- [7] Kozubal, E., Herrmann, L., Deru, M., & Clark, J. (2014, September 1). Low-Flow Liquid Desiccant Air Conditioning: General Guidance and Site Considerations. Retrieved from <https://www.osti.gov/biblio/1159352-low-flow-liquid-desiccant-air-conditioning-general-guidance-site-considerations>
- [8] Cadiau, A., Belmabkhout, Y., Adil, K., Bhatt, P. M., Pillai, R. S., Shkurenko, A., ... Eddaoudi, M. (2017, May 19). Hydrolytically stable fluorinated metal-organic frameworks for energy-efficient dehydration. Retrieved from <https://science.sciencemag.org/content/356/6339/731>
- [9] Berger, M. (2019, September 11). What is a MOF (metal organic framework)? Retrieved from <https://www.nanowerk.com/mof-metal-organic-framework.php>
- [10] Rieth, A., Yang, S., Wang, E., & Dincă, M. (2017, June 28). Record Atmospheric Fresh Water Capture and Heat Transfer with a Material Operating at the Water Uptake Reversibility Limit. Retrieved from <https://www.ncbi.nlm.nih.gov/pmc/articles/PMC5492259/>
- [11] Inglezakis, V. J., Pouloupoulos, S. G., & Kazemian, H. (2018, June 19). Insights into the S-shaped sorption isotherms and their dimensionless forms. Retrieved from <https://www.sciencedirect.com/science/article/pii/S1387181118303366#bib12>

- [12] Abtab, S., Alezi, D., Bhatt, P., Shkurenko, A., Belmabkhout, Y., Aggarwal, H., . . . Eddaoudi, M. (2018, January 11). Reticular Chemistry in Action: A Hydrolytically Stable MOF Capturing Twice Its Weight in Adsorbed Water. Retrieved from <https://www.sciencedirect.com/science/article/pii/S2451929417304734>
- [13] H. Li, W. Shi, K. Zhao, H. Li, Y. Bing, and P. Cheng, "Enhanced hydrostability in Ni-doped MOF-5," *Inorganic Chemistry*, vol. 51, no. 17, pp. 9200–9207, 2012.
- [14] Shi, B., AL-Dadah, R., Mahmoud, S., Elsayed, A., & Elsayed, E. (2016, May 19). CPO-27(Ni) metal–organic framework based adsorption system for automotive air conditioning. Retrieved from <https://www.sciencedirect.com/science/article/pii/S1359431116307773>
- [15] Fathieh, F., Kalmutzki, M., Kapustin, E., Waller, P., Yang, J., & Yaghi, O. (2018, June 8). Practical water production from desert air. Retrieved from <https://www.ncbi.nlm.nih.gov/pmc/articles/PMC5993474/>
- [16] Ehrenmann, J., Henninger, S. K., & Janiak, C. (2010, December 23). Water Adsorption Characteristics of MIL-101 for Heat-Transformation Applications of MOFs. Retrieved from <https://chemistry-europe.onlinelibrary.wiley.com/doi/10.1002/ejic.201001156>
- [17] Chemical elements by market price. (2018, October 09). Retrieved from http://www.leonland.de/elements_by_price/en/list
- [18] Kalmutzki, M. J., Diercks, C. S., & Yaghi, O. M. (2018, April 19). Metal–Organic Frameworks for Water Harvesting from Air. Retrieved from <https://onlinelibrary.wiley.com/doi/abs/10.1002/adma.201704304>
- [19] Jeremias, F., Khutia, A., Henninger, S., & Janiak, C. (2011, December 23). MIL-100(Al, Fe) as water adsorbents for heat transformation purposes-a promising application. Retrieved from <https://pubs.rsc.org/en/content/articlelanding/2012/jm/c2jm15615f>
- [20] Scientific America. (2018, November 5). A Material to Save the World? Retrieved April 20, 2020, from <https://www.scientificamerican.com/custom-media/pictet/a-material-to-save-the-world/>
- [21] Canivet, J., Fateeva, A., Guo, Y., Coasne, B., & Farrusseng, D. (2014, May 29). Water adsorption in MOFs: Fundamentals and applications. Retrieved from <https://pubs.rsc.org/en/content/articlelanding/2014/CS/C4CS00078A>
- [22] Furukawa, H., Gándara, F., Zhang, Y., Jiang, J., Queen, W., Hudson, M., & Yaghi, O. (2014, March 19). Water adsorption in porous metal-organic frameworks and related materials. Retrieved April 20, 2020, from <https://www.ncbi.nlm.nih.gov/pubmed/24588307>
- [23] Elsayed, E., AL-Dadah, R., Mahmoud, S., Elsayed, A., & Anderson, P. (2016, February 04). Aluminium fumarate and CPO-27(Ni) MOFs: Characterization and thermodynamic analysis for adsorption heat pump applications. Retrieved from <https://www.sciencedirect.com/science/article/pii/S1359431116300795>
- [24] Fröhlich, D., Henninger, S., & Janiak, C. (2014, August 26). Multicycle water vapour stability of microporous breathing MOF aluminium isophthalate CAU-10-H. Retrieved April 21, 2020, from <https://pubs.rsc.org/en/content/articlelanding/2014/dt/c4dt02264e>

- [25] Hybrid Indirect-Evaporative Modeling Project Update. (2018, April 13). Retrieved from <https://wcec.ucdavis.edu/wcec-2012-affiliates-forum-exploring-the-barriers-and-solutions-for-hvac-energy-efficiency-acceptance-15/>